# Analytical Model of a Ship's Stability on a Regular Wave

Serhii Zinchenko[1[0000−0001−5012−5029]], Oleh Tovstokoryi[1[0000−0003−3048−0028]], Kostiantyn Kyrychenko[1[0000−0002−0974−6904]], Pavlo Nosov[1[0000−0002−0974−6904]], and Ihor Popovych[2[0000−0002−1663−111X]]

[1] Kherson State Maritime Academy, Kherson, Ukraine
srz56@ukr.net
[2] Kherson State University, Kherson, Ukraine
ihorpopovych999@gmail.com

**Abstract.** One of the main dangers of sailing in storms is the change in the stability of ships due to waves, which in some cases can even lead to its overturning. Therefore, the task of constant control of the ship's stability during the voyage is an urgent scientific and technical task. A systematic approach, analysis and synthesis, methods of mathematical analysis, integral calculus, and numerical modeling were used during the research. An analytical model was developed for calculating the restoring moment in the roll channel under regular waves, depending on the geometric dimensions of the ship's hull, immersion parameters, ship motion parameters, and wave parameters. The obtained results differ from the known solutions in that they have an analytical form and can be used to assess stability in real time. The theoretical significance of the obtained results lies in the development of an analytical model for estimating stability on regular excitation. The practical value of the obtained results consists in: checking the operability of the analytical model during a computational experiment and the possibility of its use in an on-board computer of an automated or automatic control system.

**Keywords:** Intelligent transport system, analytical stability model, automatic control system, shipping safety, regular waves, restoring moment

## 1 Introduction

One of the important reasons for the safety of navigation is the reduction of the safety of vessels during passing voyage, which can be easily verified by accident statistics [3]. The reasons for the loss of stability are those that shipowners do not have reliable multi-dimensional methods for promptly assessing the reduction in stability.

In actual operation, the vessel collapses along the smooth surface of the sea and, with constant water displacement, the shape of the underwater part of the vessel's hull changes throughout the entire hour. Due to the difference in contours in the area of the cylindrical insert and at the ends of the body, it is necessary to change the contours of the current waterline, which leads to a change in the radius of the metacenter, the quiescent arm and the metacenter personal height up to 40% [3].

Research has established that the greatest danger for ships is an encounter with a wave whose length coincides with the length of the ship. When the ship is at the top of the wave (the crest of the wave coincides with the middle frame), the components of the restoring moment of the bow and stern of the hull act in the direction of the slope, trying to increase it. On the counter wave, the imaginary period of the wave decreases and the ship does not have time to react to the decrease in stability, as it is on the crest of the wave for an insignificant part of the period of its own oscillations. On a following wave, the ship changes its position relative to the wave profile and, if the speed of the ship and the wave match, it can stay on top of the wave for a long time. The master of the ship should pay attention to such operational factors as the length of the wave and the speed of its propagation. If they coincide with the length and speed of the vessel, it is necessary to change the course or reduce the speed. The works [1, 2, 4, 5, 18] give recommendations for steering a ship in following seas: the coincidence of the wavelength with the length of the ship is the most dangerous for small ships. In conditions of ocean breeze, even larger vessels can become objects of loss of stability; the shoulder of static stability significantly decreases with increasing wave height. Steep waves are more dangerous than gentle ones; the probability of loss of stability increases significantly when the ship is on the slope of the wave at speeds lower than the speed of wave propagation.

To respond to a hazard in accordance with the existing recommendations, it is first necessary to identify it, which is already a difficult technical task, since in addition to the indicated hazard, there are others that can lead to the capsize of the vessel or the destruction of the hull. For example, works [15, 16, 20] are devoted to the study of issues of hull strength. The authors of the article believe that the most radical way to avoid hazards is the use of automated systems or automatic control modules in automated systems. Examples of the use of such systems and modules are given, for example, in the authors' works [10, 17, 24–26]. The efficient operation of automated and automatic systems is ensured by mathematical models of objects or processes, which must have sufficient speed for the possibility of their use in real time. To solve problems of automatic avoidance of the stability loss, a mathematical model of stability assessment is needed, therefore the development of such a model is an urgent scientific and technical task.

The object of the research is the process of assessing stability on regular excitation.

The subject of the research is a model for assessing stability on regular excitation.

The purpose of the research is to develop an analytical model for estimating stability parameters on regular excitation for use in an on-board computer of an automated or automatic control system capable of solving the task of real-time estimation.

## 2 Problem Statement

Fig. 1 shows a lateral ship's hull projection on a regular wave.

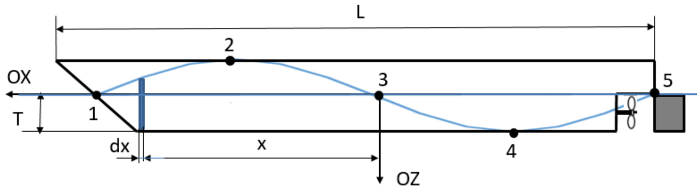


**Fig. 1.** Side projection of the ship's hull on a regular wave

The ship linked coordinate system $OXYZ$ (LCS) is shown. The geometric dimensions of the ship are specified: length $L$, width $B$, height $H$; immersion parameters: draft $T$, roll angle $\theta$; parameters of regular excitation: wavelength $\lambda$; movement parameters: vessel speed $V$ and angle of attack of the wave $q$ on the diametrical plane. It is necessary to obtain analytical dependencies of the restoring moment in the roll channel on the specified parameters for use in the on-board computer for the purpose of evaluating stability in real time in automatic control algorithms.

$$M_x = f(L, B, H, T, \theta, \lambda, V, q) \tag{1}$$

## 3 Literature Review

Many of the authors' works are devoted to the issue of development and use of mathematical models of a stationary ship on waves. In particular, in the article [23], the issue of mathematical modeling of the loss of stability of the ship during waves, under the condition of automatic course maintenance, was considered. The hydrodynamic interaction of the ship's hull, propeller, and stern was taken into account during modeling. An assessment of the heeling moment created by double rudders and propellers at different speeds was carried out, as well as the characteristics of the hydrodynamic flow around the vessel during capsizing at a critical speed were determined.

In the article [13], the mathematical model of the ship with consideration of 6 degrees of freedom, which was additionally improved to provide stability properties, was considered. The restoring moment in the roll channel was determined in real time, taking into account the characteristics of the current immersion of the hull. Dynamic forces and moments in the roll and yaw channels are calculated, taking into account the speed of movement.

Numerical forecasting of the processes of loss of stability and overturning of the ship was carried out in [12], taking into account the stability criteria of an undamaged ship. A comparative analysis of the simulation results and the conducted experiment showed that the difference between them does not exceed

3%. It was established that the cause of the ship's overturning was a significant loss of stability during free movement at high speed.

In the study [11], the processes of the ship's rocking in the roll channel with large amplitudes and the ship's capsizing due to the loss of stability were investigated. When studying the processes, the model of the ship's hull, the model of the propeller and the automatic course system maintenance were taken into account. It is established that the capsize of the ship occurs in combination with a rapid change of course, which is consistent with the results of existing model tests.

Paper [14] investigates the issues of the ship's stability loss using a mathematical model. The mathematical model includes a model of stability on course and during maneuvering. The modelling took into account the Froude - Krylov forces, hydrostatic forces and the wave pressure around the hull.

The disturbance spectrum is a key element for evaluating the behavior of a marine vessel. In the study [19] a methodology was developed and a probabilistic assessment of the disturbance spectrum was carried out by processing on-board measurements. The ocean wave is modeled using a 10-parameter bimodal spectrum combining long- and short-wavelength components. Ten parameters of the bimodal wave spectrum are determined by solving a nonlinear problem using the least squares method, which minimizes the difference between the model prediction and on-board measurement data.

In work [7] a hybrid numerical model of the vessel's free motion reaction to waves was developed, which was confirmed by experimental data. A numerical model evaluates the electromechanical conversion of wave energy by simulating the power of a tubular linear generator. Free-moving wave propulsion experiments were performed on both leading and trailing waves, using a model with sprung flaps at the bow and stern of the vessel over a range of wave frequencies.

In the study [8], a nonlinear model of the array of ship sensors was obtained and it was shown that the wave direction and wave number can be identified by at least three non-collinear sensors by analyzing the measurement results. Based on the obtained model, a Kalman filter for estimating the wave direction and wave number is built, which has a convenient structure due to the possibility of adding measurements and taking into account uncertainties. The study also evaluated the parameters of regular waves for a ship in waves with small roll and trim angles.

The article [9] investigated the reactions of small fishing vessels of different tonnage to regular waves. An increase in roll amplitude with increasing speed was found on all the studied vessels, in the presence of both oncoming and side waves. A shift of the maximum roll value to the region of long waves was observed on the oncoming wave, as the relative speed of movement increased, regardless of the vessel's size. It has been established that during sailing on oncoming and following waves, reducing the ship's speed is one of the most effective means of reducing the amplitude of oscillations in the vertical motion channel and roll channel. The roll amplitude on the wave increased rapidly only at a certain wavelength, regardless of the speed and size of the vessel.

In the study [22], a ship model was developed to study the processes of maneuvering and stability on the course. Simulations of maneuvering processes in calm water and in rough water were carried out. When comparing the obtained modeling results with experimental data, it is proven that the obtained ship model provides satisfactory forecasting of ship maneuvering processes on waves.

In work [21] developed a model of a maneuvering vessel, which includes a kinematic model of curvilinear movement and a kinematic model of steady circulation. Four scenarios obtained by combining the developed models and evaluation algorithms were matched to the maneuvering data on the navigation bridge simulator, and the consistency of the stability characteristics was verified.

The article [6] developed a method for identifying the maneuvering coefficients and the wave model based on the pivot point data and parameters of the ship's movement in calm water. Maneuvering coefficients were estimated using linear Froude-Krylov forces. Compared to known solutions, the developed method shows much better agreement with experimental data in both calm water and following seas.

## 4 Material and Method

The immersion depth of the ship's hull element $dx$, which is located at a distance $x$ from the rotation center, fig. 1, can be written as

$$z = T + A \sin\left(\frac{2\pi}{\lambda}x + \varDelta(t)\right), \tag{2}$$

where $T$ is the ship's draft, $A$ is the amplitude of the wave, $\frac{2\pi}{\lambda}$ is the frequency of the wave, reduced to the length of the ship, $\lambda$ is the length of the wave, $\varDelta(t)$ is the phase of the wave relative to the link coordinate system (LCS) of the ship

$$\varDelta(t) = -\frac{\partial \varLambda}{\partial t} = -\frac{2\pi}{T_E}t = -\frac{2\pi}{\lambda}(C + V\cos q)t, \tag{3}$$

where $C$ is the speed of wave propagation, $V$ is the ship's speed, $q$ is the course angle of the wave.

After substituting the value $\varDelta(t)$ from equation (3) into equation (2), we get

$$z = T + A \sin\left(\frac{2\pi}{\lambda}x + \frac{2\pi}{\lambda}(C + V\cos q)t\right) \tag{4}$$

Fig. 2 shows the cross-section of the ship's hull for which the wave surface passes through the ship's sides

The vessel has a roll $\theta$ to starboard. The dashed line shows the wave surface at the cross-sectional location in the absence of roll, and the solid line shows the wave surface at the cross-sectional location in the presence of roll. The surface of the wave passes through the ship's sides. Let's find the restoring moment $m_x$ of the element $dx$.

For convenience and to reduce computations, let's introduce the variable $G^*$ for the expression $\left(\frac{2\pi}{\lambda}x + \varDelta\right)$.

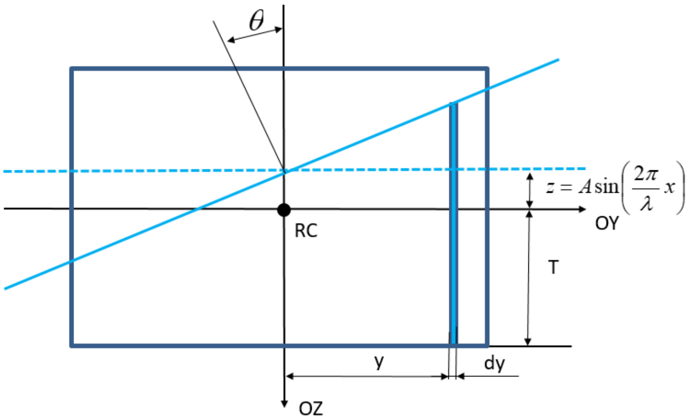


**Fig. 2.** Cross-section of the ship's hull for which the wave surface passes through the ship's sides

$$\begin{aligned}
m_x &= \rho g dx \int_{-B/2}^{B/2} zy\,dy = \rho g dx \left( \int_{-B/2}^{B/2} \left( T + A\sin G^* + y\tan\theta \right) y\,dy \right) = \\
&= \rho g dx \left( \frac{T}{2} y^2 + \frac{A}{2} \sin G^* y^2 + \frac{\tan\theta}{3} y^3 \right) \Bigg|_{-B/2}^{B/2} = \\
&= \rho g dx \left( \frac{T}{2} + \frac{A}{2} \sin G^* \left( \frac{B^2}{4} - \frac{B^2}{4} \right) + \frac{\tan\theta}{3} \left( \frac{B^3}{8} + \frac{B^3}{8} \right) \right) = \\
&= \rho g dx \frac{\tan\theta}{12} B^3
\end{aligned} \tag{5}$$

The restoring moment $M_x$ of the ship's hull is determined by integrating the obtained equation (5) along the ship's length.

$$\begin{aligned}
M_x &= \int_{-L/2}^{L/2} m_x\,dx = \rho g \frac{\tan\theta}{12} B^3 x \Bigg|_{-L/2}^{L/2} = \\
&= \rho g \frac{\tan\theta}{12} B^3 \left( \frac{L}{2} + \frac{L}{2} \right) = \\
&= \rho g \frac{\tan\theta}{12} B^3 L
\end{aligned} \tag{6}$$

In fig. 3 shows a cross-section of the ship's hull for which the wave surface passes through the ship's side and deck, as well as through the ship's side and bottom

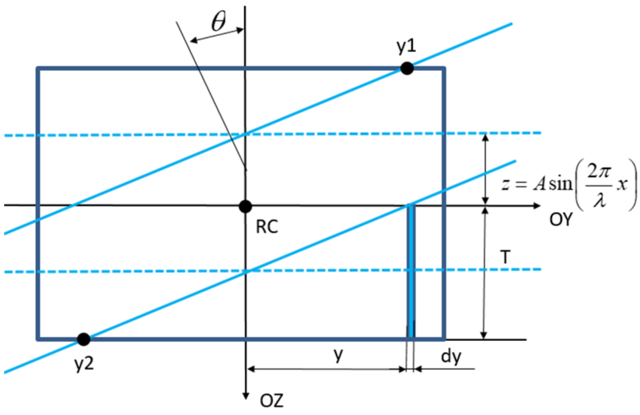


**Fig. 3.** Cross-section of the ship's hull for which the wave surface passes through the ship's side and deck, as well as through the ship's side and bottom

The coordinate of the intersection point $y_1$ of the wave surface with the ship's deck is found from the equation

$$\tan\theta y + A\sin G^* = H - T,$$

$$y_1 = \frac{1}{\tan\theta}\left(H - T - A\sin G^*\right) \tag{7}$$

and the coordinate of the intersection point $y_2$ of the wave surface with the ship's bottom is found from the equation

$$\tan\theta y + A\sin\left(\frac{2\pi}{\lambda}x + \Delta\right) = -T,$$
$$y_2 = \frac{1}{\tan\theta}\left(-T - A\sin G^*\right) \tag{8}$$

For the case when the wave crosses the port side and deck of the vessel, the restoring moment $m_x$ of the element $dx$ will have the form

$$
\begin{aligned}
m_x &= \rho g dx \int_{-B/2}^{y_1} zy\,dy + \rho g dx \int_{y_1}^{B/2} Hy\,dy = \\
&= \rho g dx \int_{-B/2}^{y_1} (T + A\sin G^* + y\tan\theta)\, y\,dy + \rho g dx\, \left.\frac{H}{2} y^2\right|_{-B/2}^{y_1} = \\
&= \rho g dx \left(\frac{T}{2} y^2 + \frac{A}{2}\sin G^* y^2 + \frac{\tan\theta}{3} y^3\right)\Bigg|_{-B/2}^{y_1} + \rho g dx \frac{H}{2}\left(\frac{B^2}{4} - y_1^2\right) \\
&= \rho g dx \left(\frac{T}{2}\left(y_1^2 - \frac{B^2}{4}\right) + \frac{A}{2}\sin G^*\left(y_1^2 - \frac{B^2}{4}\right) + \frac{\tan\theta}{3}\left(y_1^3 + \frac{B^3}{8}\right)\right) \\
&\quad + \rho g dx \frac{H}{2}\left(\frac{B^2}{4} - y_1^2\right) = \rho g dx\ y_1^2 \left(\frac{T}{2} + \frac{A}{2}\sin G^* - \frac{H}{2}\right) - \\
&- \rho g dx \frac{B^2}{4}\left(\frac{T}{2} + \frac{A}{2}\sin G^* - \frac{H}{2}\right) + \\
&\quad + \rho g dx \frac{\tan\theta}{3}\left(y_1^3 + \frac{B^3}{8}\right)
\end{aligned} \tag{9}
$$

Taking into account equation (7), we get

$$
\begin{aligned}
m_x &= -\frac{\rho g dx \tan\theta}{2} y_1^3 + \rho g dx \tan\theta \frac{B^2}{8} y_1 + \rho g dx \frac{\tan\theta}{3} y_1^3 + \rho g dx \frac{\tan\theta B^3}{8} = \\
&= \rho g dx \tan\theta \left(-\frac{1}{6} y_1^3 + \frac{B^2}{8} y_1 + \frac{B^3}{24}\right).
\end{aligned} \tag{10}
$$

For $y_1 = \frac{B}{2}$, from formula (10), we obtain formula (5), which tangentially confirms the correctness of the obtained result.

$$
\begin{aligned}
m_x &= \rho g dx \tan\theta \left(-\frac{1}{6}\left(\frac{B}{2}\right)^3 + \frac{B^2}{8}\frac{B}{2} + \frac{B^3}{24}\right) = \\
&= \rho g dx \tan\theta \left(-\frac{1}{48}B^3 + \frac{1}{16}B^3 + \frac{1}{24}B^3\right) = \\
&= \rho g dx \tan\theta \frac{B^3}{12}
\end{aligned} \tag{11}
$$

To find the restoring moment $M_x$ of the hull, it is necessary to integrate equation (10) along the length of the ship, taking into account formula (7).

$$
\begin{aligned}
M_x &= \rho g \tan\theta \int_0^L \left(-\frac{1}{6}y_1^3 + \frac{B^2}{8}y_1 + \frac{B^3}{24}\right) dx,\\
I_2 &= \frac{B^2}{8}\int_0^L y_1 dx = \frac{B^2}{8}\frac{1}{\tan\theta}\int_0^L (H - T - A\sin G^*)\, dx =\\
&= \frac{B^2}{8}\frac{(H-T)L}{\tan\theta} + \frac{B^2}{8}\frac{A}{\tan\theta}\cos\left(\frac{2\pi}{\lambda}x + \mathit{\Delta}\right)\frac{\lambda}{2\pi}\Bigg|_0^L =\\
&= \frac{B^2}{8}\frac{(H-T)L}{\tan\theta} + \frac{B^2}{8}\frac{A}{\tan\theta}\frac{\lambda}{2\pi}\left(\cos G^* - \cos(\mathit{\Delta})\right).
\end{aligned}
\tag{12}
$$

$$
\begin{aligned}
I_1 &= -\frac{1}{6}\int_0^L y_1^3\, dx = -\frac{1}{6t^3\theta}\int_0^L (H - T - AG^*)^3\, dx\\
&- \frac{1}{6t^3\theta}\int_0^L (H-T)^3 dx + \frac{3(H-T)^2 A}{6t^3\theta}\int_0^L \sin G^* dx\\
&- \frac{3(H-T)A^2}{6t^3\theta}\int_0^L \sin^2 G^* dx + \frac{A^3}{6t^3\theta}\int_0^L \sin^3 G^* dx
\end{aligned}
\tag{13}
$$

All integrals used in formula (13) can be found from the tabular integrals

$$
\begin{aligned}
&\int_0^L (H-T)^3\, dx = (H-T)^3 L,\\
&\int_0^L \sin G^* dx = \frac{\lambda}{2\pi}\left(\cos(\mathit{\Delta}) - \cos\left(\frac{2\pi L}{\lambda} + \mathit{\Delta}\right)\right),\\
&\int_0^L \sin^2\ G^* dx = \frac{L}{2} - \frac{\lambda}{8\pi}\left(\sin\left(\frac{4\pi L}{\lambda} + 2\mathit{\Delta}\right) - \sin(2\mathit{\Delta})\right),\\
&\int_0^L \sin^3 G^* dx = \frac{3\lambda L}{8\pi} - \frac{\lambda}{2\pi}\left(\cos(\mathit{\Delta}) - \cos\left(\frac{2\pi L}{\lambda} + \mathit{\Delta}\right)\right)\\
&\qquad + \frac{\lambda}{6\pi}\left(\cos^3(\mathit{\Delta}) - \cos^3\left(\frac{2\pi L}{\lambda} + \mathit{\Delta}\right)\right).
\end{aligned}
\tag{14}
$$

After substituting tabular integrals (14) into formula (13), we get

$$
\begin{aligned}
I_1 &= -\frac{1}{6}\frac{1}{\tan^3\theta}(H-T)^3 L + 3\frac{(H-T)^2 A}{6\tan^3\theta}\left(-\frac{\lambda}{2\pi}\cos G^* - \cos(\mathit{\Delta})\right)\\
&- 3\frac{(H-T)A^2}{6\tan^3\theta}\left(\frac{L}{2} - \frac{\lambda}{8\pi}\sin\left(\frac{4\pi L}{\lambda} + 2\mathit{\Delta}\right) - \sin(2\mathit{\Delta})\right)\\
&+ \frac{A^3}{6\tan^3\theta}\left(-\frac{\lambda}{2\pi}(\cos G^* - \cos(\mathit{\Delta})) + \frac{\lambda}{6\pi}(\cos^3 G^* - \cos^3(\mathit{\Delta}))\right),\\
I_3 &= \frac{B^3}{24}L,\\
M_x &= \rho g \tan\theta (I_1 + I_2 + I_3).
\end{aligned}
\tag{15}
$$

For the case when the wave crosses the starboard side and the bottom of the vessel, the restoring moment $m_x$ of the element $dx$ will have the form. To simplify the formal expression, let's introduce the variable $R^*$ which will be equal to: $\left(\frac{B}{4}^2 - y_2^2\right)$.

$$
\begin{aligned}
m_x &= \rho g dx \int_{y_2}^{B/2} zydy = \rho g dx \int_{y_2}^{B/2} (T + A \sin G^* + y \tan\theta)\, ydy = \\
&= \rho g dx \left(\frac{T}{2} y^2 + \frac{A}{2} \sin G^* y^2 + \frac{\tan\theta}{3} y^3\right)\Bigg|_{y_2}^{B/2} = \\
&= \rho g dx \left(\frac{T}{2}\ R^* + \frac{A}{2} \sin G^* R^* + \frac{\tan\theta}{3} R^*\right) \\
&= -\rho g dx y_2^2 \left(\frac{T}{2} + \frac{A}{2} G^*\right) + \rho g dx \frac{B^2}{4} \left(\frac{T}{2} + \frac{A}{2} \sin G^*\right) + \\
&\quad + \rho g dx \frac{\tan\theta}{3} \left(\frac{B^3}{8} - y_2^3\right) = \\
&\frac{\rho g dx \tan\theta}{2} y_2^3 - \rho g dx \tan\theta \frac{B^2}{8} y_2 - \rho g dx \frac{\tan\theta}{3} y_2^3 + \\
&\quad + \rho g dx \frac{\tan\theta}{3} \frac{B^3}{8} \quad = \rho g dx \tan\theta \left(\frac{1}{6} y_2^3 - \frac{B^2}{8} y_2 + \frac{B^3}{24}\right).
\end{aligned}
\tag{16}
$$

For $y_2 = -\frac{B}{2}$, from formula (16) we get formula (5), which tangentially confirms the correctness of the obtained result.

$$
\begin{aligned}
m_x &= \rho g dx \tan\theta \left(\frac{1}{6}\left(-\frac{B}{2}\right)^3 - \frac{B^2}{8}\left(-\frac{B}{2}\right) + \frac{B^3}{24}\right) = \\
&= \quad \rho g dx \tan\theta B^3 \left(-\frac{1}{48} + \frac{1}{16} + \frac{1}{24}\right) = \rho g dx \tan\theta \frac{B^3}{12}
\end{aligned}
\tag{17}
$$

The restoring moment of the hull $M_x$ is found by integrating formula (16) along the length of the vessel

$$
M_x = \rho g \tan\theta \int_0^L \left(\frac{1}{6} y_2^3 - \frac{B^2}{8} y_2 + \frac{B^3}{24}\right) dx \tag{18}
$$

$$
\begin{aligned}
I_2 &= -\frac{B^2}{8} \int_0^L y_2\, dx = -\frac{B^2}{8} \frac{1}{tan\theta} \int_0^L (-T - A \sin G^*)\, dx = \\
&= \frac{B^2}{8} \frac{TL}{tan\theta} - \frac{B^2}{8} \frac{A}{tan\theta} \cos G^* \frac{\lambda}{2\pi}\Bigg|_0^L = \\
&= \frac{B^2}{8} \frac{TL}{tan\theta} - \frac{B^2}{8} \frac{A}{tan\theta} \frac{\lambda}{2\pi} (\cos G^* - \cos(\mathit{\Delta}))
\end{aligned}
\tag{19}
$$

$$
\begin{aligned}
I_1 = \frac{1}{6}\int_0^L y_2^3\,dx = \frac{1}{6}\frac{1}{\tan^3\theta}\int_0^L (-T - A\sin G^*)^3\,dx = \\
= -\frac{1}{6}\frac{1}{\tan^3\theta}\int_0^L T^3\,dx - 3\frac{T^2 A}{6\tan^3\theta}T^2 A\int_0^L \sin G^*\,dx - \\
- 3\frac{T^2 A}{6\tan^3\theta}\int_0^L \sin^2 G^*\,dx - \frac{A^3}{6\tan^3\theta}\int_0^L \sin^3 G^*\,dx
\end{aligned}
\tag{20}
$$

After substituting the tabular integrals (14), we get

$$
\begin{aligned}
I_1 = -\frac{1}{6}\frac{1}{\tan^3\theta}T^3 L - 3\frac{T^2 A}{6\tan^3\theta}\left(\frac{-\lambda}{2\pi}(\cos G^* - \cos\Delta)\right) - \\
- 3\frac{TA^2}{6\tan^3\theta}\left(\frac{L}{2} - \frac{\lambda}{8\pi}\left(\sin\left(\frac{4\pi}{\lambda}L + 2\Delta\right) - \sin 2\Delta\right)\right) - \\
- \frac{1}{6}\frac{A^3}{\tan^3\theta}\left(-\frac{\lambda}{2\pi}(\cos G^* - \cos\Delta) + \frac{\lambda}{6\pi}\left(\cos^3 G^* - \cos^3\Delta\right)\right)
\end{aligned}
\tag{21}
$$

$$
I_3 = \int_0^L \frac{B^3}{24}dx = \frac{B^3}{24}L
$$

$$
M_x = \rho g \tan\theta (I_1 + I_2 + I_3)
$$

In fig. 4 shows a cross-section of the ship's hull for which the wave surface passes through the deck and bottom of the vessel

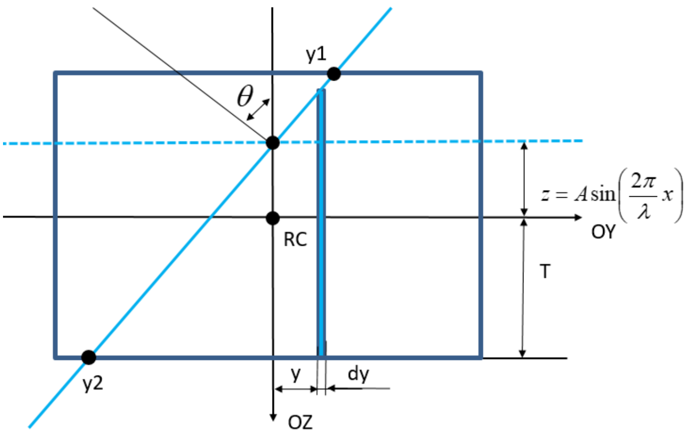


**Fig. 4.** Cross-section of the ship's hull for which the wave surface passes through the deck and bottom of the vessel

The restoring moment $m_x$ of the element $dx$ for this case is equal to
Taking into account equations (7), (8), we get

$$\begin{aligned}
m_x &= \rho g dx \int_{y_2}^{y_1} z y dy + \rho g dx \int_{y_1}^{B/2} H y dy = \\
&= \rho g dx \int_{y_2}^{y_1} \left( T + A \sin\left(\frac{2\pi}{\lambda} x + \Delta\right) + y \tan\theta \right) y dy + \\
&+ \rho g dx \cdot \frac{H}{2} y^2 \Big|_{y_1}^{B/2} = \\
&= \rho g dx \cdot \left( \frac{T}{2}\left(y_1^2 - y_2^2\right) + \frac{A}{2} \sin G^* y^2 + \frac{\tan\theta}{3}\left(y_1^3 - y_2^3\right) \right) + \\
&+ \rho g dx \cdot \frac{H}{2}\left(\frac{B^2}{4} - y_1^2\right) = \\
&= \rho g dx \cdot y_1^2 \left( \frac{T}{2} + \frac{A}{2} \sin G^* - \frac{H}{2} \right) - \\
&- \rho g dx \cdot y_2^2 \left( \frac{T}{2} + \frac{A}{2} \sin G^* \right) + \\
&+ \rho g dx \cdot \frac{HB^2}{4} - \rho g dx \cdot \frac{\tan\theta}{3}\left(y_1^3 - y_2^3\right)
\end{aligned} \tag{22}$$

$$\begin{aligned}
m_x = &- \frac{1}{2} \rho g dx \cdot y_1^3 \tan\theta + \frac{1}{2} \rho g dx \cdot y_2^3 \tan\theta + \rho g dx \cdot \frac{HB^2}{8} + \\
&+ \rho g dx \cdot \frac{\tan\theta}{3}\left(y_1^3 - y_2^3\right) = \\
&= \rho g dx \cdot \tan\theta \left( -\frac{y_1^3}{6} + \frac{y_2^3}{6} \right) + \rho g dx \cdot \frac{HB^2}{8}
\end{aligned} \tag{23}$$

For $y_1 = -\frac{B}{2}$, $y_2 = -\frac{B}{2}$, taking into account that $\frac{H}{B} = \tan(\theta)$, from formula (23) we obtain formula (5), which tangentially confirms the correctness of the obtained result.

$$\begin{aligned}
m_x &= \rho g dx \tan\theta \left( -\frac{y_1^3}{6} + \frac{y_2^3}{6} \right) + \rho g dx \cdot \frac{HB^2}{8} = \\
&= \rho g dx \tan\theta \left( -\frac{B^3}{48} - \frac{B^3}{48} \right) + \rho g dx \tan\theta \cdot \frac{B^3}{8} \\
&= \rho g dx \tan\theta B^3 \left( -\frac{1}{24} + \frac{1}{8} \right) = \rho g dx \tan\theta \cdot \frac{B^3}{12}
\end{aligned} \tag{24}$$

The restoring moment of the hull $M_x$ is found by integrating formula (23) along the length of the vessel

$$M_x = \rho g \tan\theta \int_0^L \left( -\frac{1}{6} y_1^3 + \frac{1}{6} y_2^3 \right) dx + \rho g \int_0^L \frac{HB^2}{8} dx \tag{25}$$

Formulas for calculating the integral $I_1 = -\frac{1}{6}\int_0^L y_1^3\,dx$ and the integral $I_2 = -\frac{1}{6}\int_0^L y_2^3\,dx$ were found earlier, see formulas (13) and (20).

$$I_3 = \frac{HB^2}{2\cdot 4}\int_0^L dx = \frac{HB^2}{8}L \tag{26}$$

$$M_x = \rho g \tan\theta(I_1 + I_2) + \rho g I_3 \tag{27}$$

Variants of the wave surface and hull location can be different along the length of the vessel, therefore, when integrating, it is necessary to take this into account and choose the necessary formula according to the situation.

## 5 Experiment, Results and Discussion

To check the performance of the developed model, a computational experiment was conducted. Characteristics of the ship, movement parameters and turbulence are given in Table 1.

**Table 1.** Characteristics of the vessel

| **Parameter name** | **Value** |
|---|---|
| Length of the vessel $L$, m | 100 |
| Width of the vessel $B$, m | 13 |
| Height of the vessel $H$, m | 10 |
| Draft $T$, m | 4 |
| Ship's roll teta, dg | 40 |
| The amplitude of the wave $A$, m | 4 |
| Wavelength, $\lambda$ | 100 |

The results of the computational experiment are shown in Fig. 5.

The graphs show the change in the restoring moment $M_x$ during integration along the length of the ship, the dependence $y_1(x)$ of the intersection point position of the wave surface with the ship deck on the cross-section coordinate, and the dependence $y_2(x)$ of the intersection point position of the wave surface with the ship bottom on the cross-section coordinate for roll angles $\theta = 10dg$ (green curve), $\theta = 30dg$ (blue curve) and $\theta = 60dg$ (red curve). For the vessel's characteristics listed in Table 1, the port side coordinate is $y_1 = -\frac{B}{2} = -6.5\,m$, the starboard coordinate is $y_r = \frac{B}{2} = 6.5\,m$. For the roll angle $\theta = 10dg$ (green curve): the intersection point coordinate of the wave surface with the ship's deck is in the range $10 \leq y_1(x) \leq 55$, outside the starboard side $y_1(x) > 6.5$.

This means that the wave surface in all sections crosses the starboard side of the vessel; the intersection point coordinate of the wave surface with the ship's bottom varies in the range $-45 \leq y_2(x) \leq 0$, depending on the cross-section coordinate, it can be located both within the ship's hull and outside the port side. This means that the wave surface for different cross-section crosses both

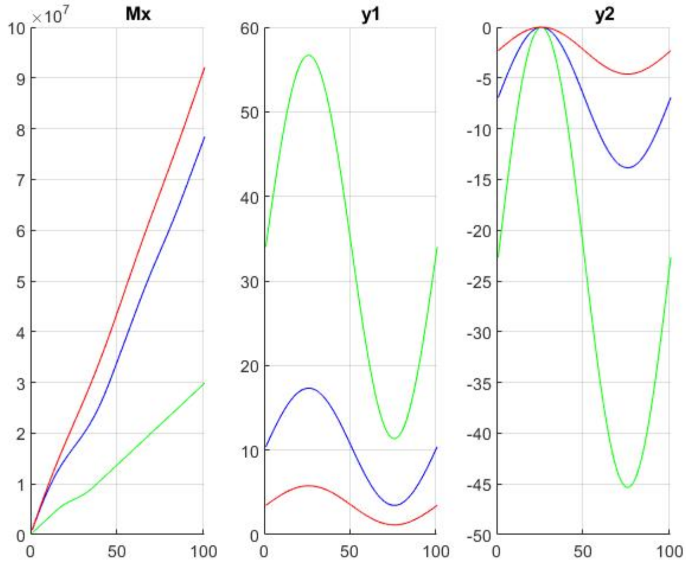


**Fig. 5.** Results of the computational experiment

the bottom and the port side of the vessel. For the roll angle $\theta = 30dg$ (blue curve): the intersection point coordinate of the wave surface with the ship's deck is in the range $5 \leq y_1(x) \leq 17$, i.e., depending on the cross-section coordinate, it can cross both the deck and the starboard side of the ship; the intersection point coordinate of the wave surface with the ship's bottom is in the range $-14 \leq y_2(x) \leq 0$, i.e., depending on the cross-section coordinate, it can cross both the bottom and the port side of the ship. For the roll angle $\theta = 60dg$ (red curve): the intersection point coordinate of the wave surface with the ship's deck is in the range $0 \leq y_1(x) \leq 5$, that is, it always crosses the ship's deck; the intersection point coordinate of the wave surface with the ship's bottom is in the range $-5 \leq y_2(x) \leq 0$, that is, it always crosses the ship's bottom. A change in the intersection variant leads to a change in the value of the restoring moment $m_x$ of the element $dx$ and the intensity of moment accumulation $M_x(x)$ during integration.

The total restoring moment $M_x$ for roll angle $\theta = 10dg$ is $M_x = 3.0 \times 10^7$ Nm, for roll angle $\theta = 30dg$ is $M_x = 7.8 \times 10^7$ Nm, for roll angle $\theta = 60dg$ is $M_x = 9.2 \times 10^7$ Nm. The dependencies of the restoring moment $M_x$ on the roll angle $\theta$ for the wave amplitudes $A = 0$m (blue graph), $A = 2$m (green graph) and $A = 4$m (red graph) are shown in Fig. 6

In Fig. 7, the dependence of the restoring moment $M_x$ in the roll channel on the displacement of the wave $\Delta(t)$ relative to the ship's hull is shown, see equation (3), for roll angles $\theta = 10dg$, $\theta = 30dg$, and $\theta = 60dg$. As can be seen from the graphs, the restoring moment varies depending on the wave phase (wave position) relative to the ship's hull, it has the smallest value for the wave

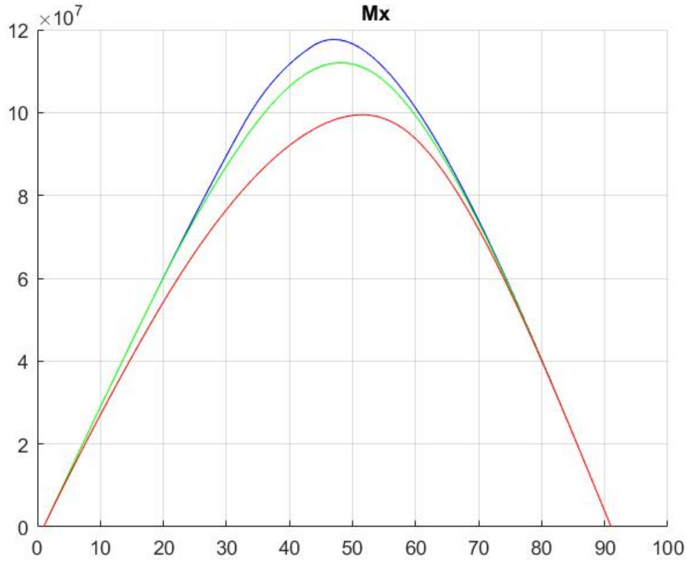


**Fig. 6.** Dependences of the restoring moment $\boldsymbol{M_x}$ on the roll angle $\boldsymbol{\theta}$ for the wave amplitudes $\boldsymbol{A = 0}$ m, $\boldsymbol{A = 2}$ m and $\boldsymbol{A = 4}$ m

phase $\Delta(t) = 90dg$ and $\Delta(t) = 270dg \ = -90dg$ when the ship is on the crest of the wave. The periodic change of the restoring moment is the cause of such a dangerous phenomenon as parametric resonance.

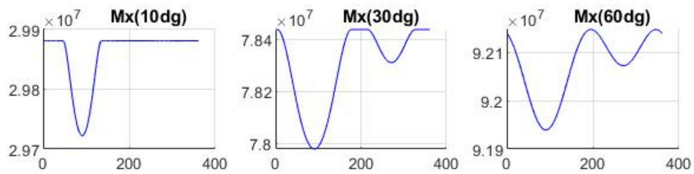


**Fig. 7.** Dependence of the restoring moment $M_x$ in the roll channel on the displacement of the wave $\Delta(t)$ relative to the ship's hull

Figure 8 shows the dependence of the restoring moment $M_x$ in the roll channel on the wavelength $\lambda$ for the roll angle $\theta = 10dg$.

As can be seen from the obtained results, the restoring moment has slight fluctuations with an amplitude of up to 0.7% for wavelengths less than a third of the ship's length, then the amplitude increases to 3% for a wavelength equal to the ship's length. For wavelengths that are several times longer than the length of the vessel, $\lambda > (3-4)L$, the relative increase in the restoring moment is up to 7%.

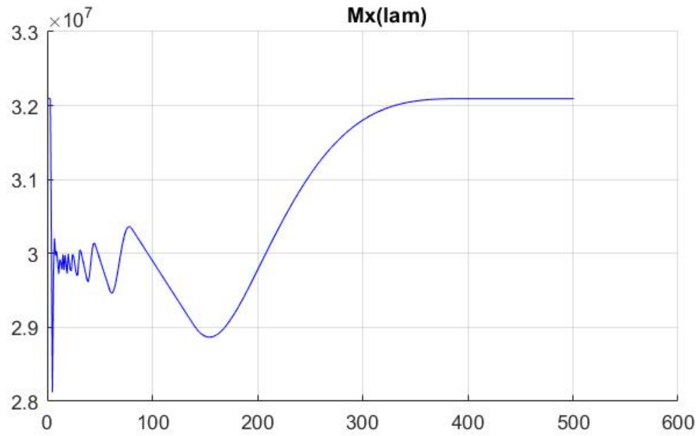


**Fig. 8.** Dependence of the restoring moment $M_x$ in the roll channel on the wavelength $\lambda$

## 6 Conclusions

An analytical model for calculating the restoring moment in the ship's roll channel for regular waves has been developed, depending on the geometric dimensions of the ship's hull, immersion parameters, ship movement parameters and wave parameters. The obtained results are explained by: the possibility of analytically finding the restoring moment $m_x$ of the cross-sections for different cases of immersion; the possibility of analytically finding the restoring moment $M_x$ of the entire hull by integrating the restoring moments $m_x$ of the cross-sections along the length of the ship. The obtained results differ from known solutions in that they have an analytical form. They are reproducible and can be used to study the stability of the vessel in waves, as well as in the on-board computer of an automated or automatic system.

The theoretical significance of the obtained results lies in the development of an analytical model for calculating the restoring moment in the roll channel of a ship under regular waves.

The practical value of the obtained results consists in: checking the performance of the developed model during the computational experiment; the possibility of using an analytical model in an on-board computer of an automated or automatic control system to evaluate the stability characteristics of a vessel in real time.

## References

1. Recommendation on intact stability for passenger and cargo ships under 100 meters in length. Tech. Rep. RESOLUTION A.167 (ES.IV), IMCO (11 1968)

2. Recommendation on a severe wind and rolling criterion (weather criterion) for the intact stability of passenger and cargo ships of 24 meters in length and over. Tech. Rep. RESOLUTION A.562(14), IMO (11 1985)
3. Why do ships built in compliance with the laws of stability capsize? Tech. Rep. 113 (1985)
4. Guidance to the master for avoiding dangerous situations in following and quartering seas. Tech. Rep. MSC/Circ.707, IMO (1995)
5. Revised guidance to the master for avoiding dangerous situations in adverse weather and sea conditions. Tech. Rep. MSC.1/Circ.1228, IMO (2007)
6. Araki, M., Sadat, H., Sanada, Y., Umeda, N., Stern, F.: Improved Maneuvering-Based Mathematical Model for Free-Running Ship Motions in Following Waves Using High-Fidelity CFD Results and System-Identification Technique: Risk of Capsizing, pp. 91–115 (01 2019). https://doi.org/10.1007/978-3-030-00516-0-6
7. Bowker, J.: Coupled dynamics of a flapping foil wave powered vessel. Ph.D. thesis, Thesis submitted for the degree of Doctor of Philosophy (2018)
8. Dirdal, J.A., Skjetne, R., Rohac, J., Fossen, T.I.: Online wave direction and wave number estimation from surface vessel motions using distributed inertial measurement arrays and phase-time-path-differences. Ocean Engineering **249**(3), 110760 (2022). https://doi.org/10.1016/j.oceaneng.2022.110760
9. Im, N., Lee, S.M.: A study on motion response of small fishing vessels according to various tonnage in regular waves. Journal of the Korean Society of Marine Environment and Safety **27**(6), 832–838 (2021). https://doi.org/10.7837/kosomes.2021.27.6.832
10. Krugliy, D., Appazov, E., Zinchenko, S., Nosov, P.: Choice of the fractal method for visualization of input data while designing support systems for decision-making by navigator. Science and Innovation **17**(5), 63–72 (2021). https://doi.org/10.15407/scine17.05.063
11. Liu, L., Feng, D., Wang, X., Zhang, Z., Yu, J., Chen, M.: Study on extreme roll event with capsizing induced by pure loss of stability for the free-running onr tumblehome. Ocean Engineering **257**(4), 111656 (2022). https://doi.org/10.1016/j.oceaneng.2022.111656
12. Liu, L., Yao, C., Feng, D., Wang, X., Yu, J., Chen, M.: Numerical study of the interaction between the pure loss of stability, surf-riding, and broaching on ship capsizing. Ocean Engineering **266**(4), 112868 (2022). https://doi.org/10.1016/j.oceaneng.2022.112868
13. Lu, J., Gu, M., Boulougouris, E.: Further study on one of the numerical methods for pure loss of stability in stern quartering waves. Journal of Marine Science and Engineering **11**(2), 394 (2023). https://doi.org/10.3390/jmse11020394
14. Lu, J., Gu, M., Boulougouris, E.: A unified numerical method for broaching and loss of stability in astern seas. Journal of Marine Science and Engineering **11**(8), 1555 (2023). https://doi.org/10.3390/jmse11081555
15. Marasanov, V., Stepanchikov, D., Sharko, A., Sharko, O.: Operator of the dynamic process of the appearance of acoustic emission signals during deforming the structure of materials. In: 2020 IEEE 40th International Conference on Electronics and Nanotechnology (ELNANO). pp. 646–650 (2020). https://doi.org/10.1109/ELNANO50318.2020.9088893
16. Marasanov, V., Stepanchikov, D., Sharko, A., Sharko, O.: Technology for determining the residual life of metal structures under conditions of combined loading according to acoustic emission measurements. In: Communications in Computer and Information Science, vol. 1158, pp. 202–217. Springer (2020). https://doi.org/10.1007/978-3-030-61656-4-13

17. Nosov, P., Koretsky, O., Zinchenko, S., Prokopchuk, Y., Gritsuk, I., Sokol, I., Kyrychenko, K.: Devising an approach to safety management of vessel control through the identification of navigator's state. Eastern-European Journal of Enterprise Technologies **4**(3(124)), 19–32 (2023). https://doi.org/10.15587/1720-4061.2023.286156
18. Okada, Takuzo, C.: Marine Weather Ship Handling in Rough Sea. No. 45 in P&I Loss Prevention Bulletin, Japan P&I Club (2019)
19. Park, M.J., Kim, Y.: Probabilistic estimation of directional wave spectrum using onboard measurement data. Journal of Marine Science and Technology **29**, 200–220 (2024). https://doi.org/10.1007/s00773-023-00984-z
20. Sharko, M., Liubchuk, O., Krapivina, G., Petrushenko, N., Gonchar, O., Vorobyova, K., Vasylenko, N.: Information technology to assess the enterprises' readiness for innovative transformations using markov chains. In: Lecture Notes on Data Engineering and Communications Technologies, vol. 149, pp. 197–213. Springer (2023). https://doi.org/10.1007/978-3-031-16203-9
21. Wang, Y., Perera, L.P., Batalden, B.M.: Kinematic motion models based vessel state estimation to support advanced ship predictors. Ocean Engineering **286**, 115503 (2023). https://doi.org/10.1016/j.oceaneng.2023.115503
22. Xie, Z., Falzarano, J.M., Wang, H.: A framework of numerically evaluating a maneuvering vessel in waves. Journal of Marine Science and Engineering **8**, 392 (2020). https://doi.org/10.3390/jmse8060392
23. Zeng, K., Lu, J., Gu, M., Yang, C.: A comparative analysis of cfd and the potential flow method for the pure loss of stability in following waves. Journal of Marine Science and Engineering **11**(11), 2135 (2023). https://doi.org/10.3390/jmse11112135
24. Zinchenko, S., Kobets, V., Tovstokoryi, O., Kyrychenko, K., Nosov, P., Popovych, I.: Control of the pivot point position of a conventional single-screw vessel. In: CEUR Workshop Proceedings. vol. 3513, pp. 130–140 (2023), https://ceur-ws.org/Vol-3513/paper11.pdf
25. Zinchenko, S., Kobets, V., Tovstokoryi, O., Nosov, P., Popovych, I.: Intelligent system control of the vessel executive devices redundant structure. In: CEUR Workshop Proceedings. vol. 3403, pp. 582–594 (2023), https://ceur-ws.org/Vol-3403/
26. Zinchenko, S., Kyrychenko, K., Grosheva, O., Nosov, P., Popovych, I., Mamenko, P.: Automatic reset of kinetic energy in case of inevitable collision of ships. In: 13th International Conference on Advanced Computer Information Technologies (ACIT). pp. 496–500. IEEE Xplore (2023). https://doi.org/10.1109/ACIT58437.2023.10275545